Molecular Dynamics Study of a Carbon Nanotube Binding Reversible Cyclic Peptide

Chi-cheng Chiu, Marie C. Maher, Gregg R. Dieckmann, and Steven O. Nielsen*

Department of Chemistry and Alan G. MacDiarmid NanoTech Institute, The University of Texas at Dallas, 800 West Campbell Road, Richardson, Texas 75080

ARTICLE

ABSTRACT Many potential biological applications of single-walled carbon nanotubes (SWNTs) require their dispersion in aqueous conditions. Recently, Dieckmann *et al.* designed a series of reversible cyclic peptides (RCPs) which exist in linear or cyclized states through controlled formation of an intramolecular disulfide bond between terminal Cys residues. These RCP-Cys peptides have been shown to disperse SWNTs in aqueous solution and form peptide/SWNT complexes which are stable against dilution. However, the detailed molecular interactions between the peptide and the SWNT in an aqueous environment remain unexplored. Here, fully atomistic molecular dynamics simulations were used to study the effect of RCP-Cys at the water/SWNT interface. We show that the peptide—SWNT association is thermodynamically favorable through free energy calculations. Furthermore, we analyze the structure and energetics of the possible β-sheet-like ring stacking that can form on the SWNT through peptide backbone hydrogen bonding. Our results reveal the thermodynamic driving force for the formation of an ordered, self-assembled RCP-Cys/SWNT complex, which provides insight into peptide design strategies for future applications.

KEYWORDS: carbon nanotube · cyclic peptide · hydrogen bonding · molecular dynamics · free energy

The unique mechanical, electrical, and optical properties of single-walled carbon nanotubes (SWNTs) suggest their potential in a variety of applications. In particular, numerous applications are envisaged in biomedicine such as tissue supports, artificial muscles, and cancer treatment.[1−4] In order to use SWNTs in bioapplications, however, there are currently two major obstacles that must be overcome: (1) the heterogeneous mixture of as-synthesized SWNTs must be separated to obtain the nanotube type of interest, and (2) SWNTs are intrinsically insoluble in aqueous media.

To overcome these problems, Dieckmann *et al.* synthesized reversible cyclic peptides (RCPs) and used them to effect limited diameter-selective dispersion of SWNTs.[5,6] The RCP design was inspired by the cyclic peptide (CP) nanotubes of Ghadiri and co-workers.[7−9] Using amino acids of alternating L- and D-chirality, cyclic peptides can adopt a planar conformation in which the side chains point radially outward, leaving the center open.[7,8,10] Dieckmann *et al.* utilized this cavity to accommodate a SWNT, thereby dispersing SWNTs in aqueous solution. The key difference between Dieckmann's RCPs and Ghadiri's CPs is the presence of a reversible disulfide bond, which allows for switching between linear and cyclized states through disulfide reduction or oxidation, respectively. The original RCP design had the sulfur atoms incorporated directly into the peptide backbone, whereas a newer design (RCP-Cys) uses terminal cysteine residues (Cys) to form the disulfide bond, simplifying the peptide synthesis.[11] RCP-Cys peptides are first introduced into solution as linear peptides and then oxidized to the cyclized state during sonication in the SWNT dispersion procedure. Once the RCP-Cys has cyclized around the SWNT, the SWNT is protected from contacting water and thereby dispersed in aqueous solution.

There are numerous advantages to using reversible cyclic peptides as SWNT dispersion agents: (1) after cyclization around a SWNT through disulfide bond formation, RCP-Cys peptides are unable to dissociate from the SWNT under nonreducing conditions, leading to extremely stable SWNT dispersions;[11] (2) RCP-Cys peptides avoid the biological compatibility problems associated with the use of detergents;[12] (3) the length of the RCP-Cys controls the diameter of the SWNT around which the RCP-Cys cyclizes, providing SWNT diameter selectivity which is potentially limited by peptide polymerization through interpeptide disulfide bond formation;[6,13] (4) the noncovalent modification of a SWNT by RCP-Cys preserves the intrinsic optical, mechanical, and conductive properties of the

*Address correspondence to steven.nielsen@utdallas.edu.

Received for review October 23, 2009 and accepted April 21, 2010.

Published online April 27, 2010.
10.1021/nn901484w

SWNT; and (5) the radial conformation of the RCP-Cys side chains provides a wealth of coupling points for further functionalization, for example, by antibodies for biological targeting. The disulfide "lock" prevents peptide removal from the nanotube, which is especially important when considering applications in which the peptide solution concentration would change, such as introduction into a biological system. However, there are some unanswered questions as to the behavior of the RCP-Cys/SWNT systems at the molecular level, such as the thermodynamic driving force for RCP-Cys peptides to associate with the SWNT surface, and the exact self-assembled peptide structure on the SWNT surface. One possible macromolecular structure would be a RCP-Cys−nanotube encasing the SWNT. The RCP-Cys−nanotube could be formed by stacking of RCP-Cys peptides through interpeptide backbone hydrogen bonding, similar to what is observed for CPs. However, CP−nanotubular structures only form in apolar solvent, which is different in character from the SWNT/water interface considered here.

In this paper, we used molecular dynamics (MD) simulations to study the interaction between one member of the RCP-Cys family of peptides (namely, RC5-Cys which contains 13 amino acids) and a (13,0) SWNT (10.2 Å in diameter measured between carbon centers). The peptide−SWNT interaction was characterized through its van der Waals (vdW) energy. Hydrogen bonds (H-bonds) formed between the peptide and water or between water molecules were quantified through geometric analysis. The radial distribution function of water around the SWNT was used to study the effect of the RCP-Cys on disrupting the ordered water in proximity to the hydrophobic SWNT surface. Furthermore, calculation of the peptide−SWNT association free energy showed that the peptide−SWNT interaction overcomes the unfavorable peptide conformational entropy change upon association with SWNTs. Combined with calculation of the peptide−peptide dimerization free energy, we conclude that the formation of a RCP-Cys−nanotube macromolecular complex containing a SWNT within its central pore is thermodynamically favorable.

RESULTS AND DISCUSSION

Peptide−SWNT Interaction. To characterize the peptide−SWNT interaction, we began with an equilibrium MD simulation of one RC5-Cys peptide around an infinitely long (13,0) SWNT. RC5-Cys has the amino acid sequence Ac-CY(^{D}AK)$_4$^{D}AQC−CONH$_2$, where Ac and CONH$_2$ indicate N-terminal acetylation and C-terminal amidation, respectively. The amino acids are represented by their single-letter abbreviations, where residues with D-chirality are denoted with the superscript D. The two terminal Cys residues were oxidized to form a disulfide bond, resulting in a cyclized peptide. As shown in Figure 1a−c, at equilibrium, the peptide backbone is in close contact with the SWNT and the peptide side chains radiate outward from the SWNT and interact with water. RC5-Cys has an average vdW interaction of ∼−62 kcal/mol with the SWNT (data not shown). Approximately 60% of this vdW energy is contributed by the peptide backbone due to its close contact with the SWNT surface. This vdW interaction provides a favorable enthalpic contribution for the peptide−SWNT interaction.

It is known that, in the presence of a SWNT, water structures into layers.[15] In this report, a two-dimensional radial distribution function (RDF) between water molecules and the nanotube, $g_{yz}(r)$, was used to study the effect of RC5-Cys on such a layered structure. This RDF measures the water density as a function of the distance, r, from the nanotube long axis. The two distinct peaks of the RDF in the bare SWNT region (see Figure 2) suggest that water molecules form two distinct layers on the SWNT surface. However, in the peptide-coated region, the water structuring is significantly attenuated. We also evaluated the pair entropy (entropy contribution due to particle pair correlations) between the SWNT and water, $S^{(2)}_{NT,wt}$.[16−19] This is obtained by integrating the two-dimensional RDF, $-0.525k_B \int_0^\infty r g_{yz}(r) \ln(g_{yz}(r)) dr$, where k_B is the Boltzmann constant, as described in detail in the Methods section. The resulting $S^{(2)}_{NT,wt}$ for the bare SWNT region is $-6.67k_B$, compared with that for the peptide-coated SWNT region of $+7.04k_B$. A comparison of the pair entropies suggests that, after peptide cyclization around the SWNT, the peptide can interact with water molecules and disrupt the water layering, contributing a favorable entropic change to the peptide−SWNT association. However, the pair entropy estimation is only part of the overall system entropy. To evaluate the total entropy change, more simulation data would be required. One method to compute the total entropy change is to calculate the peptide−SWNT association free energy at two different temperature ($\pm\Delta T$) and use $\Delta S(T) = (\Delta G(T + \Delta T) - \Delta G(T - \Delta T))/2\Delta T$.[20] This method is computationally expensive and beyond the scope of our study.

RC5-Cys can form H-bonds with nearby water molecules while cyclized around the SWNT. In this study, we evaluated the number of H-bonds formed in the cylindrical layer within 5 Å of the peptide and 3.5 Å from the SWNT side wall, corresponding to the first water layer (shown by the RDF analysis in Figure 2) around the SWNT. The H-bonds counted in this layer include water−water and water−peptide H-bonds. The total number of H-bonds was then normalized by the layer length along the SWNT long axis. In addition, the average H-bond donor (hydrogen atoms) to acceptor (oxygen and nitrogen atoms) ratio in the layer (⟨donor⟩/⟨acceptor⟩ where ⟨ ⟩ represents a time average) was also calculated to further analyze the available H-bonding sites. The resulting number of H-bonds per unit length

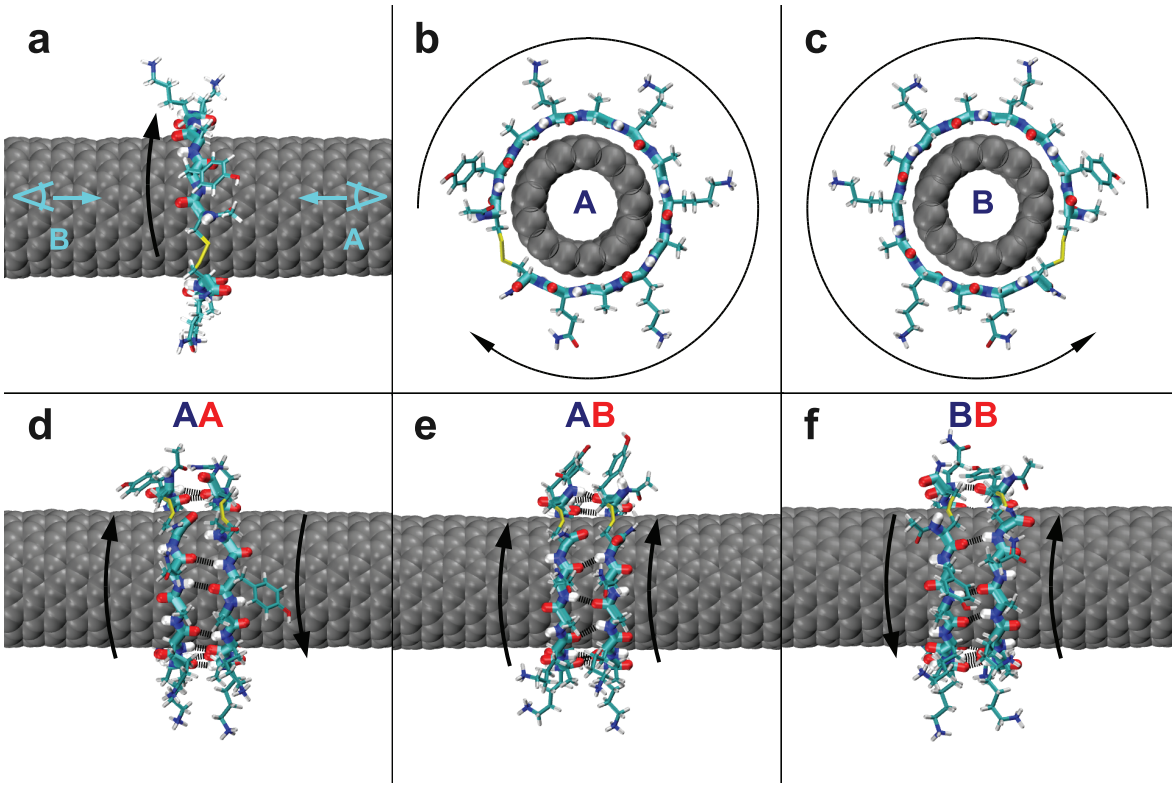

Figure 1. Representative RC5-Cys−SWNT configurations from the MD simulations of the single RC5-Cys system (a−c) and the RC5-Cys dimer systems (d−f). For panels a, d, e, and f, the systems are viewed perpendicular to the SWNT long axis. Panels b and c display two different views down the SWNT long axis (perpendicular to panel a), to illustrate the "A" and "B" faces of the peptide. Depending on the A/B face combination, the dimer structures can be categorized as AA, AB, or BB stacking, corresponding to panels d, e, and f, respectively. The arrows represent the N- to C-terminal direction for each peptide. In an antiparallel β-sheet-like structure, the two arrows point in opposite directions (d,f), whereas in a parallel β-sheet-like structure, the two arrows point in the same direction (e). The peptide is visualized using a stick model, and the SWNT is shown using a vdW model. H-bonds between adjacent peptide backbones are drawn using black dashed lines. Water molecules have been removed for clarity. Images were created using VMD.[14]

(Figure 3) is greater in the peptide-coated region than in the bare SWNT region, although there are fewer water molecules in the peptide-coated region due to the presence of the peptide. The peptide backbone provides H-bonding donors (N−H) and acceptors (C═O) which compensate for the loss of water molecules due to volume exclusion by RC5-Cys. As a result, more H-bonding sites were found in the peptide-coated layer (⟨donor⟩/⟨acceptor⟩ = 48/55) compared with the bare SWNT region (⟨donor⟩/⟨acceptor⟩ = 44/44). This suggests that the peptide can locally induce more H-bond formation, thereby alleviating the unfavorable water/SWNT interfacial energy. Such a H-bonding ability with water also distinguishes the RCP-Cys family from common surfactants, such as sodium dodecyl sulfate, which cannot form H-bonds using the parts that mainly interact with the SWNT (usually their hydrophobic regions). Note, however, that this picture is for a single RC5-Cys molecule on a SWNT. We will discuss the interaction between adjacent RC5-Cys peptides on a SWNT surface in detail later.

After cyclization around the SWNT, the only way for RCP-Cys to dissociate from the SWNT without breaking the disulfide bond is to slide off the SWNT end. To estimate the peptide−SWNT association free energy, we performed a series of constrained MD simulations to calculate the free energy of sliding a cyclized RC5-Cys off the end of a (13,0) SWNT with a finite length of 42.7 Å. Figure 4 displays the resulting free energy (ΔG) profile along with the change in vdW energy between the peptide and the SWNT (E_{vdW}) as a function of the peptide−SWNT center of mass (COM) separation distance (denoted d_{PN}). The overall RC5-Cys−SWNT association free energy (ΔG_{CMD}) is −12.1 kcal/mol, suggesting a favorable interaction between RC5-Cys and the SWNT. For $0 < d_{PN} < 19$ Å, where the peptide is cyclized around the SWNT, ΔG increases accompanying the increase of E_{vdW} as the peptide moves toward the SWNT end. This suggests that ΔG is mainly composed of E_{vdW} when the peptide is cyclized on the SWNT. At $d_{PN} = 20$ Å, both ΔG and E_{vdW} decrease because the peptide partially loses contact with the SWNT and adjusts its conformation to maximize the vdW interaction with the SWNT. In the range $21 \leq d_{PN} \leq 33$ Å, where the peptide is within 12 Å of the SWNT end, the free energy profile has large variations due to the conformational adjustments of the peptide at the nanotube edge. However, because free energy is a state function, the

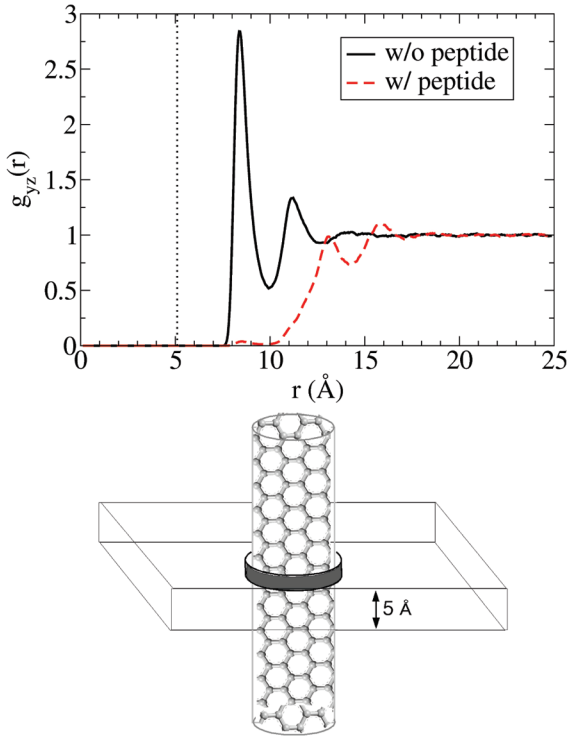

Figure 2. Two-dimensional RDF between the water oxygen atoms and the nanotube long axis. RDF for the bare SWNT region is shown as a black solid line, and that for the RC5-Cys-coated region is shown as a red dashed line. The dotted line indicates the position of the SWNT side wall. The schematic drawing at the bottom illustrates a SWNT with a single RC5-Cys (gray ring) cyclized around it, as well as the water slab (with a 5 Å thickness and centered at the peptide COM) used for the RDF calculation of the peptide-coated region as described in detail in the Methods section.

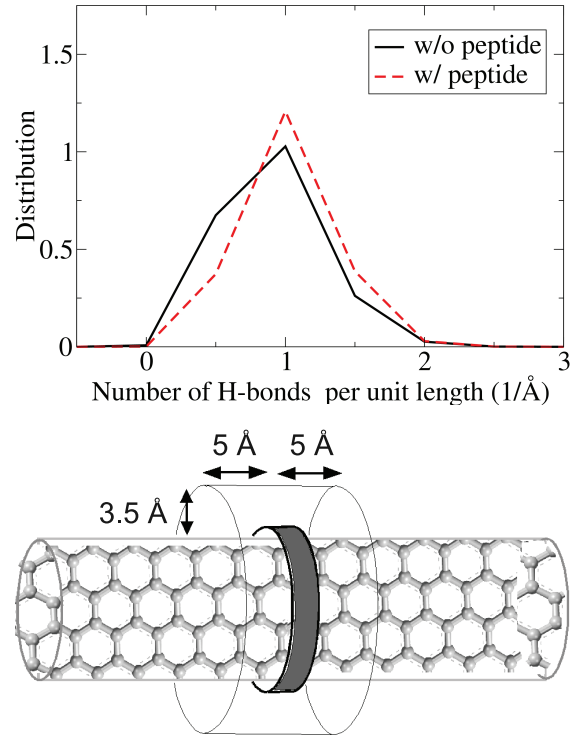

Figure 3. Distributions of the number of H-bonds per unit length for a 3.5 Å thick water layer along a SWNT. Data for the bare SWNT are drawn as a black solid line, and those for the peptide-coated region as a red dashed line. The schematic drawing at the bottom illustrates a SWNT with a single RC5-Cys (gray ring) cyclized around it, as well as the cylindrical shell region (3.5 Å in thickness, 10 Å in length, and centered at the peptide COM) used for the H-bond number analysis as described in the text.

overall free energy difference between the states of RC5-Cys being on (d_{PN} = 0 Å) *versus* off (d_{PN} = 50 Å) the SWNT is representative of the peptide−SWNT association free energy.

The peptide backbone has more conformational freedom in solution than when cyclized around the SWNT. This results in an entropic penalty to the overall RC5-Cys−SWNT association free energy. However, according to the RDF analysis (Figure 2), the entropically favorable release of structured water due to the peptide−SWNT association counterbalances the loss of peptide entropy.[21] In addition, as shown in Figure 3, RC5-Cys can form H-bonds with water molecules and reduce the interfacial energy of the water/SWNT interface. The peptide backbone also has favorable vdW interactions with the SWNT side wall. These provide the system favorable enthalpic and entropic changes and compensate the unfavorable peptide conformational entropy. The resulting ΔG_{CMD} of −12.1 kcal/mol suggests that the overall RC5-Cys−SWNT association is thermodynamically favorable.

Peptide−Peptide Stacking Interaction. When cyclized around the SWNT, RC5-Cys participates not only in H-bonding interactions with water molecules but also with neighboring RC5-Cys peptides to form β-sheet-like structures. A cyclized RCP-Cys in its planar conformation has two faces. In this study, we distinguished between these two faces as follows: viewed along the SWNT long axis, if the N- to C-terminus direction (following the peptide backbone) of the peptide is clockwise, as illustrated in Figure 1b, we denote it as the "A" face; if counter-clockwise, it is denoted as the "B" face (Figure 1c). Hence, a cyclized peptide can use one face to interact with the adjacent peptide on one side and the other face to interact with another peptide. The peptide stacking structure depends on the orientation of adjacent peptides. It is similar to an antiparallel β-sheet if two peptides form AA or BB stacking (Figure 1d,f), whereas it is similar to a parallel β-sheet if the dimer is in the AB stacking conformation (Figure 1e). Figure 5 illustrates the time evolution and distribution of the number of H-bonds formed between two peptide backbones for the three different stacking conformations. The AA and BB stacking have similar H-bond distributions, whereas the AB stacking forms fewer H-bonds. The main difference between the antiparallel and parallel β-sheet conformations is the H-bond pattern. In the antiparallel β-sheet structure (AA and BB stacking), interbackbone H-bonds are equally spaced, and the atoms participating in each H-bond are aligned (Figure 6a). Conversely, in the AB parallel β-sheet struc-

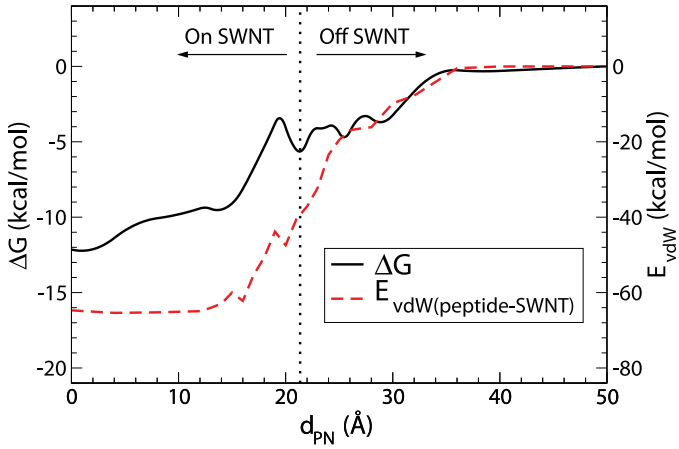

Figure 4. RC5-Cys−SWNT association free energy (black solid line) and vdW energy (red dashed line) profile as a function of the peptide−SWNT COM separation distance, d_{PN}. The left and right *y*-axes represent the free energy and vdW energy, respectively. The vertical black dashed line indicates the position of the SWNT end.

ture, the interbackbone H-bonds are formed at an angle (Figure 6b). Angled H-bonds make it harder to align two peptide backbones to maximize the number of H-bonds, which suggests less effective H-bonding than in the antiparallel β-sheet conformation. The resulting number of H-bonds for AB stacking is smaller than that for AA and BB stacking, making AB stacking less energetically favorable than AA and BB stacking.

We calculated the dimerization free energies for the three possible peptide−peptide stackings (AA, AB, and BB) using constrained MD. Figure 7 illustrates the free energy profile for the three stacking conformations as a function of the distance between the two peptide COMs (d_{PP}). All three conformations show two minima separated by a free energy barrier. These 4−7 kcal/mol free energy barriers are caused by the disruption of the water cage structure surrounding each isolated peptide. After overcoming the solvent cage barrier, the free energy of the AA stacking reaches its minimum at 4.8 Å with a free energy change (ΔG_{AA}) of −10.9 kcal/mol. For BB stacking, the free energy approaches its minimum at 5.1 Å with ΔG_{BB} of −9.1 kcal/mol. The difference between ΔG_{AA} and ΔG_{BB} is ∼1.8 kcal/mol, which is approximately the energy of one N−H···O H-bond.[22] This agrees with the H-bond analysis shown in Figure 5, where the average number of H-bonds in AA stacking is one more than in BB stacking. As for AB stacking, the free energy reaches its first minimum at ∼7.4 Å with $\Delta G = -6.1$ kcal/mol before the solvent cage barrier. After breaking the solvent cage, the AB stacking conformation begins forming, and the resulting free energy reaches its minimum at 5.1 Å with ΔG_{AB} of −5.6 kcal/mol. Note that the AB stacking free energy ($\Delta G_{AB} = -5.6$ kcal/mol) is close to the free energy minimum at ∼7.4 Å ($\Delta G = -6.1$ kcal/mol), which suggests that the free energy gained from forming H-bonds between adjacent peptide backbones is offset by the energy cost of breaking the peptide solvent cages. Comparing the three stacking conformations, AA and BB stacking are thermodynamically more stable than AB stacking. Moreover, from the peptide−SWNT free energy data, RC5-Cys has a favorable interaction with the SWNT. As illustrated in Figure 8, the combined free energy data suggest that it is thermodynamically favorable for the RC5-Cys peptides to interact with the SWNT and form peptide stacks along the SWNT long axis in an antiparallel β-sheet-like conformation; this would be the most probable structure if sufficient surface sampling occurs. Note that the results presented throughout the article are equilibrium in nature and hence do not allow us to comment on a

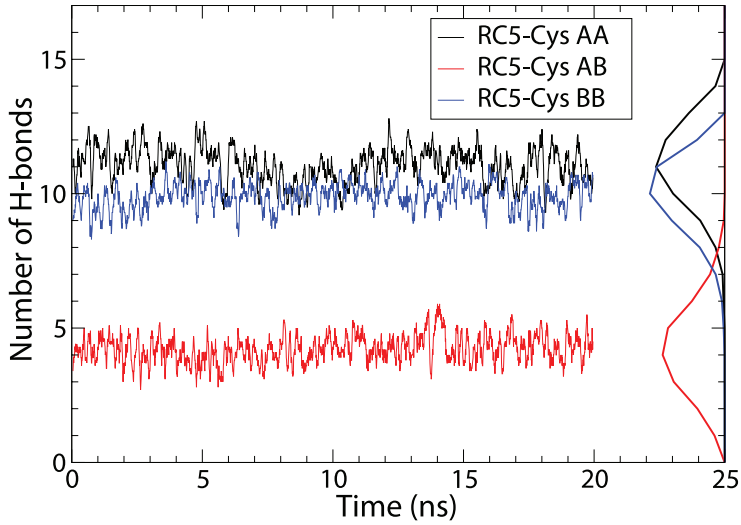

Figure 5. Time evolution of the number of H-bonds formed between two adjacent RC5-Cys backbones. The distributions of the H-bond number are shown on the right edge of the graph. Data for the AA, AB, and BB stacking conformations are illustrated in black, red, and blue, respectively.

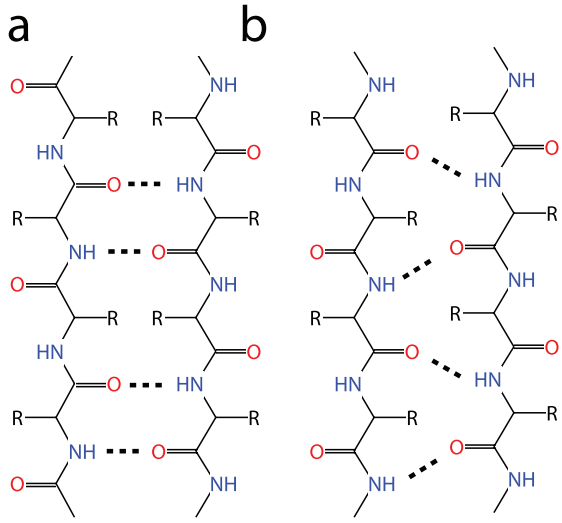

Figure 6. Schematic illustration of the H-bond patterns in (a) an antiparallel β-sheet and (b) a parallel β-sheet. The H-bonds between adjacent peptide backbones are drawn using dashed lines.

possible mechanism for peptide association with a SWNT.

CONCLUSIONS

In this study, we investigated the noncovalent functionalization of a SWNT by reversible cyclic peptides using MD simulations. While cyclizing around a (13,0) SWNT, 60% of the RC5-Cys−SWNT vdW energy is contributed from the peptide backbone. Also, the presence of RC5-Cys peptides disrupts the distinct water layers around the nanotube and locally increases the number density of H-bonds. The above factors give rise to a favorable enthalpic and entropic change which compensates the unfavorable peptide conformational change after cyclization around a SWNT. The peptide−SWNT association free energy calculation gives a favorable ΔG_{CMD} of −12.1 kcal/mol. Furthermore, RC5-Cys peptides can form H-bonds with adjacent peptide backbones and self-assemble into peptide stacks along the SWNT. Depending on the relative orientations of adjacent peptides, the peptide stacking can be antiparallel β-sheet-like (AA and BB) or parallel β-sheet-like (AB) with different H-bonding patterns. The RC5-Cys dimerization free energies ΔG_{AA}, ΔG_{BB}, and ΔG_{AB} are −10.9, −9.1, and −5.6 kcal/mol, respectively. This suggests that the peptides can stack along the SWNT and preferentially form antiparallel β-sheet-like structures if sufficient surface sampling occurs. Combining the peptide stacking free energy and the peptide−SWNT association free energy data (Figure 8), we suggest that forming RC5-Cys tubular peptide stacks encasing the SWNT is a thermodynamically favorable process.

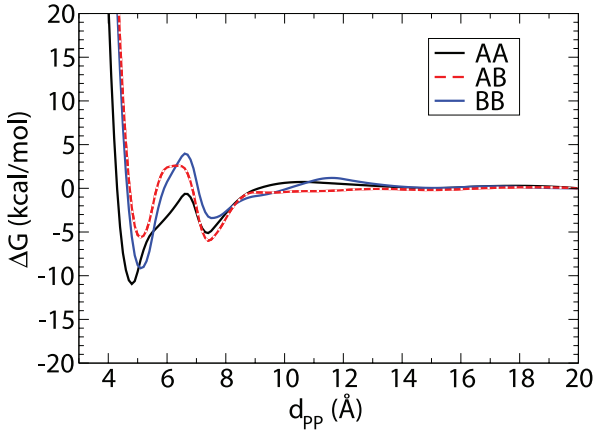

Figure 7. Dimerization free energy profiles as a function of the peptide−peptide COM separation distance, d_{PP}. Profiles for the AA, AB, and BB stacking conformations are illustrated in black, red, and blue, respectively.

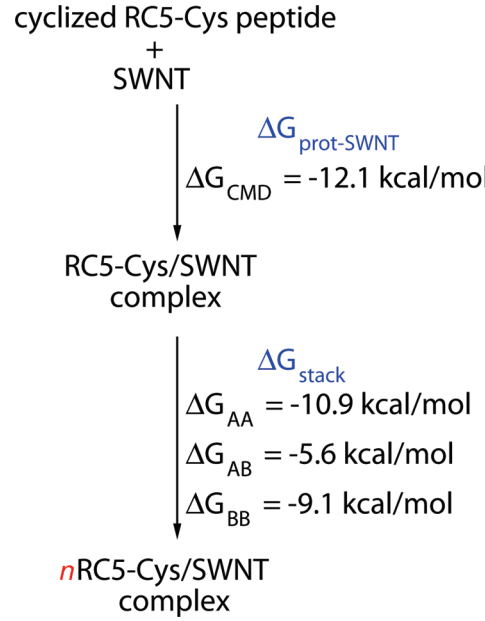

Figure 8. Thermodynamic data show favorable interactions between RC5-Cys and a SWNT, and between two cyclized peptides on a SWNT. Importantly, this diagram does not imply that RC5-Cys cyclizes before associating with a SWNT.

One of the reasons to use RCP-Cys to disperse SWNTs is that RCP-Cys provides limited SWNT diameter selectivity depending on the peptide length.[6] Such diameter selectivity for the RCP family was probed by Friling *et al.* using all-atom MD simulations, where they explored the possible formation of peptide dimers due to interpeptide disulfide bonds.[13] As first suggested by Dieckmann *et al.*, interpeptide disulfide bond formation would likely lead to peptide polymerization.[6] In such a peptide polymer, however, a RCP-Cys monomer would still likely form H-bonds with other peptide monomers and form similar tubular peptide stacks as reported in this study. Unfortunately, a study of the effect of peptide polymerization on the SWNT diameter selectivity of RCP-Cys would be difficult for all-atom MD (as used in this study and in Friling's work) due to size- and time-scale limitations. More efficient approaches, such as coarse-grained (CG) MD, are better suited to probe the behavior of large-scale RCP-Cys−SWNT systems; CG

force fields that can accurately describe the interactions within the peptide−SWNT complexes would need to be developed. Indeed, one of the current paradigms in CG force field parametrization is to use experimental or all-atom MD free energy data—the work described in this paper is therefore useful to develop and validate CG force fields.[23,24] The data presented here not only reveal the fundamental thermodynamic properties of the RCP-Cys−SWNT system and give insight into future peptide design and applications but also provide a basis for future large-scale modeling studies of related systems.

METHODS

Molecular Dynamics Simulations. The initial RC5-Cys coordinates were generated by mutating the terminal groups of the previously reported RC5 model into Cys residues.[6] The resulting amino acid sequence is Ac-CY(^{D}AK)$_4$^{D}AQC−CONH$_2$, where Ac and CONH$_2$ indicate N-terminal acetylation and C-terminal amidation, respectively; the residues are represented by their single-letter abbreviations; D-amino acids are denoted with the superscript D. The two terminal Cys residues were oxidized to form a disulfide bond, resulting in the cyclized form of RC5-Cys. A (13,0) SWNT with 15 cell replications (10.2 Å in diameter and 64.0 Å in length, measured from carbon atom centers) was used for all simulations if not otherwise stated. To create an infinitely long SWNT, the SWNT terminal carbons shared chemical bonds, and the *x*-dimension of the simulation unit cell was set to be equal to the SWNT length. The long axis of the nanotube was immobilized on the *x*-axis by adding an elastic force (1 kcal/mol/Å^2 force constant with the nanotube radius as its equilibrium distance) between each nanotube carbon atom and the *x*-axis to prevent the nanotube from bending or tilting. Water molecules were excluded from the nanotube interior. The SWNT carbon atoms were modeled using the aromatic sp^2 carbon parameters from the CHARMM27 force field.[25]

Simulations were carried out using the NAMD package version 2.6b[26] with the CHARMM27 force field[25] for 20 ns if not otherwise stated. The pressure was controlled at 1 atm by the Nosé−Hoover Langevin piston method, and the temperature was retained at 300 K using Langevin dynamics.[27,28] Three-dimensional periodic boundary conditions were applied, and the electrostatic interactions were evaluated using the particle mesh Ewald method. The TIP3P model was used for water molecules in all simulations.[29] Bonds between hydrogen atoms and heavy atoms were constrained at their equilibrium lengths using the SHAKE/RATTLE algorithm.[30,31] A 2 fs time step was used to integrate the equations of motions. System coordinates were saved every 10 ps for data analysis.

Radial Distribution Functions. The two-dimensional RDF, $g_{yz}(r)$, was evaluated between the oxygen atom of each water molecule and the long axis of the SWNT (which is also the *x*-axis in this study). Water molecules within a layer of 5 Å thickness, perpendicular to the SWNT long axis, and centered at COM of the peptide were used to calculate the water−SWNT RDF in the peptide-coated SWNT region.

Pair Entropy Analysis. Using the RDF data, the pair entropy, $S^{(2)}_{\alpha,\beta}$, can be estimated by applying the following equation:[16−19]

$$\frac{S^{(2)}_{\alpha,\beta}}{k_B} = -\frac{\rho}{2}\int_0^\infty dV[g_{\alpha,\beta}(r)\ln(g_{\alpha,\beta}(r))] \quad (1)$$

where k_B is the Boltzmann constant, ρ is the number density of the system, and $g_{\alpha,\beta}(r)$ is the RDF between components α and β. Here, the pair entropy between the SWNT and water was evaluated by integrating the two-dimensional SWNT−water RDF, $g_{yz}(r)$, over a cylindrical volume:

$$\frac{S^{(2)}_{NT,wt}}{k_B} = -h\pi\rho\int_0^\infty rg_{yz}(r)\ln(g_{yz}(r))dr \quad (2)$$

where *h* is the height of the cylinder, which was chosen to be 5 Å (see Figure 2). We assume that the number density of water, ρ = 0.0334 Å^{-3}, is unaffected by the presence of RC5-Cys and the SWNT. Thus, $S^{(2)}_{NT,wt}$ can be evaluated through

$$S^{(2)}_{NT,wt} = -0.525k_B\int_0^\infty rg_{yz}(r)\ln(g_{yz}(r))dr \quad (3)$$

The value of this integral is reported in the Results and Discussion section.

H-Bond Analysis. In this study, a H-bond was defined as follows: for a hydrogen attached to a heteroatom A, a H-bond is formed with another heteroatom B only if the distance between the two heavy atoms ($\overline{AB}$) is smaller than 4 Å and the angle formed by atoms A, H, and B (A−H−B) is larger than 150°.[32]

Peptide−SWNT Association Free Energy Calculations. In the RC5-Cys−SWNT association free energy calculations, a finite (13,0) SWNT with 10 cell replications, 42.7 Å in length, was used. The SWNT long axis was aligned and constrained on the *x*-axis as described above. Thus, d_{PN} can be calculated using only *x*-component values. Twenty-six simulations of 10 ns each were performed by constraining the peptide−SWNT distance to a fixed d_{PN} value with a harmonic spring of stiffness 200 kcal/mol/Å^2. The 26 constraint values were 0, 4, 8, 12, 13, 14, ..., 26, 27, 28, 30, 32, 36, 40, 45, and 50 Å; more constraint points were used near the nanotube edge at ~21 Å. The resulting mean force of constraint *versus* distance function was integrated to yield the free energy profile. This profile can be viewed as the free energy change for the process of sliding the peptide off the SWNT. The peptide−SWNT association free energy (ΔG_{CMD}) is then the free energy difference between the RC5-Cys on (d_{PN} = 0 Å) and off (d_{PN} = 50 Å) the SWNT. In simulations with an infinitely long SWNT, no water molecules were located inside the SWNT. Therefore, to be consistent and prevent water from diffusing into the finite SWNT used for this calculation, the SWNT was capped at both ends. To our knowledge, no cap structures for (13,0) have been reported. Thus, instead of building SWNT caps, we simply added two carbon atoms (one at either end of the SWNT) and constrained them on the *x*-axis. Additional harmonic forces were applied to constrain these two carbon atoms at the SWNT edges. Because the SWNT was also constrained on the *x*-axis, these two carbon atoms served as SWNT caps and blocked water from entering the SWNT. More than one carbon atom could instead have been added at each SWNT edge, which would change the free energy profile. However, free energy is a state function, and our main interest is the free energy difference between RC5-Cys on *versus* off the SWNT. Therefore, these capping atoms do not affect the ΔG_{CMD} value.

Peptide Dimerization Free Energy Calculations. The three possible peptide dimerization free energies (ΔG_{AA}, ΔG_{BB}, and ΔG_{AB}) were estimated using the constrained MD method as a function of the COM separation distance between two peptides (d_{PP}). Again, with the SWNT long axis constrained on the *x*-axis, d_{PP} can be represented using only *x*-components. Seventeen simulations of 6 ns each were performed by constraining two peptides at a fixed d_{PP} value using a harmonic spring constant of 200 kcal/mol/Å^2. The 17 constraint values were 4, 4.5, 5, ..., 7.5, 8, 9, 10, 11, 12, 14, 16, 18, and 20 Å. The resulting mean force of constraint *versus* distance function was then integrated to give the free energy profile.

Acknowledgment. The authors acknowledge the Donors of the American Chemical Society Petroleum Research Fund (S.O.N.) and a grant from the Human Frontier Science Program (G.R.D.; Grant RGY0070/2005-C) for partial support of this research. The authors thank D. Moore for technical assistance. The authors would also like to acknowledge the Texas Advanced Computing Center (TACC) at The University of Texas at Austin for provid-

ing HPC resources that have contributed to the research results reported within this paper.

REFERENCES AND NOTES

1. Baughman, R. H.; Zakhidov, A. A.; de Heer, W. A. Carbon Nanotubes—The Route toward Applications. *Science* **2002**, *297*, 787–792.
2. Kam, N. W. S.; O'Connell, M.; Wisdom, J. A.; Dai, H. J. Carbon Nanotubes as Multifunctional Biological Transporters and Near-Infrared Agents for Selective Cancer Cell Destruction. *Proc. Natl. Acad. Sci. U.S.A.* **2005**, *102*, 11600–11605.
3. Liu, Z.; Tabakman, S.; Welsher, K.; Dai, H. J. Carbon Nanotubes in Biology and Medicine: *In Vitro* and *In Vivo* Detection, Imaging and Drug Delivery. *Nano Res.* **2009**, *2*, 85–120.
4. Chakravarty, P.; Marches, R.; Zimmerman, N. S.; Swafford, A. D. E.; Bajaj, P.; Musselman, I. H.; Pantano, P.; Draper, R. K.; Vitetta, E. S. Thermal Ablation of Tumor Cells with Anti Body-Functionalized Single-Walled Carbon Nanotubes. *Proc. Natl. Acad. Sci. U.S.A.* **2008**, *105*, 8697–8702.
5. Ortiz-Acevedo, A.; Dieckmann, G. R. Synthesis of Reversible Cyclic Peptides. *Tetrahedron Lett.* **2004**, *45*, 6795–6798.
6. Ortiz-Acevedo, A.; Xie, H.; Zorbas, V.; Sampson, W. M.; Dalton, A. B.; Baughman, R. H.; Draper, R. K.; Musselman, I. H.; Dieckmann, G. R. Diameter-Selective Solubilization of Single-Walled Carbon Nanotubes by Reversible Cyclic Peptides. *J. Am. Chem. Soc.* **2005**, *127*, 9512–9517.
7. Ghadiri, M. R.; Granja, J. R.; Milligan, R. A.; Mcree, D. E.; Khazanovich, N. Self-Assembling Organic Nanotubes Based on a Cyclic Peptide Architecture. *Nature* **1993**, *366*, 324–327.
8. Hartgerink, J. D.; Clark, T. D.; Ghadiri, M. R. Peptide Nanotubes and Beyond. *Chem.—Eur. J.* **1998**, *4*, 1367–1372.
9. Fernandez-Lopez, S.; Kim, H. S.; Choi, E. C.; Delgado, M.; Granja, J. R.; Khasanov, A.; Kraehenbuehl, K.; Long, G.; Weinberger, D. A.; Wilcoxen, K. M.; *et al.* Antibacterial Agents Based on the Cyclic D,L-α-Peptide Architecture. *Nature* **2001**, *412*, 452–455.
10. Khurana, E.; Nielsen, S. O.; Ensing, B.; Klein, M. L. Self-Assembling Cyclic Peptides: Molecular Dynamics Studies of Dimers in Polar and Nonpolar Solvents. *J. Phys. Chem. B* **2006**, *110*, 18965–18972.
11. Becraft, E. J.; Klimenko, A. S.; Dieckmann, G. R. Influence of Alternating L-/D-Amino Acid Chiralities and Disulfide Bond Geometry on the Capacity of Cysteine-Containing Reversible Cyclic Peptides To Disperse Carbon Nanotubes. *Biopolymers* **2009**, *92*, 212–221.
12. Dietrich, C.; Volovyk, Z. N.; Levi, M.; Thompson, N. L.; Jacobson, K. Partitioning of Thy-1, Gm1, and Cross-Linked Phospholipid Analogs into Lipid Rafts Reconstituted in Supported Model Membrane Monolayers. *Proc. Natl. Acad. Sci. U.S.A.* **2001**, *98*, 10642–10647.
13. Friling, S. R.; Notman, R.; Walsh, T. R. Probing Diameter-Selective Solubilisation of Carbon Nanotubes by Reversible Cyclic Peptides Using Molecular Dynamics Simulations. *Nanoscale* **2010**, *2*, 98–106.
14. Humphrey, W.; Dalke, A.; Schulten, K. VMD—Visual Molecular Dynamics. *J. Mol. Graphics* **1996**, *14*, 33–38.
15. Walther, J. H.; Jaffe, R.; Halicioglu, T.; Koumoutsakos, P. Carbon Nanotubes in Water: Structural Characteristics and Energetics. *J. Phys. Chem. B* **2001**, *105*, 9980–9987.
16. Hernando, J. A. Thermodynamic Potentials and Distribution-Functions I. A General Expression for the Entropy. *Mol. Phys.* **1990**, *69*, 319–326.
17. Lazaridis, T.; Paulaitis, M. E. Entropy of Hydrophobic Hydration—A New Statistical Mechanical Formulation. *J. Phys. Chem.* **1992**, *96*, 3847–3855.
18. Lazaridis, T.; Paulaitis, M. E. Simulation Studies of the Hydration Entropy of Simple, Hydrophobic Solutes. *J. Phys. Chem.* **1994**, *98*, 635–642.
19. Kinoshita, M.; Matubayasi, N.; Harano, Y.; Nakahara, M. Pair-Correlation Entropy of Hydrophobic Hydration: Decomposition into Translational and Orientational Contributions and Analysis of Solute-Size Effects. *J. Chem. Phys.* **2006**, *124*, 024512.
20. van Gunsteren, W. F.; Bakowies, D.; Baron, R.; Chandrasekhar, I.; Christen, M.; Daura, X.; Gee, P.; Geerke, D. P.; Glattli, A.; Hunenberger, P. H.; *et al.* Biomolecular Modeling: Goals, Problems, Perspectives. *Angew. Chem., Int. Ed.* **2006**, *45*, 4064–4092.
21. Whitesides, G. M.; Mathias, J. P.; Seto, C. T. Molecular Self-Assembly and Nanochemistry—A Chemical Strategy for the Synthesis of Nanostructures. *Science* **1991**, *254*, 1312–1319.
22. Vargas, R.; Garza, J.; Friesner, R. A.; Stern, H.; Hay, B. P.; Dixon, D. A. Strength of the N−H···O═C and C−H···O═C Bonds in Formamide and *N*-Methylacetamide Dimers. *J. Phys. Chem. A* **2001**, *105*, 4963–4968.
23. DeVane, R.; Shinoda, W.; Moore, P. B.; Klein, M. L. Transferable Coarse Grain Nonbonded Interaction Model for Amino Acids. *J. Chem. Theory Comput.* **2009**, *5*, 2115–2124.
24. Shinoda, W.; Devane, R.; Klein, M. L. Multi-Property Fitting and Parameterization of a Coarse Grained Model for Aqueous Surfactants. *Mol. Simul.* **2007**, *33*, 27–36.
25. MacKerell, A. D.; Bashford, D.; Bellott, M.; Dunbrack, R. L.; Evanseck, J. D.; Field, M. J.; Fischer, S.; Gao, J.; Guo, H.; Ha, S.; *et al.* All-Atom Empirical Potential for Molecular Modeling and Dynamics Studies of Proteins. *J. Phys. Chem. B* **1998**, *102*, 3586–3616.
26. Phillips, J. C.; Braun, R.; Wang, W.; Gumbart, J.; Tajkhorshid, E.; Villa, E.; Chipot, C.; Skeel, R. D.; Kale, L.; Schulten, K. Scalable Molecular Dynamics with NAMD. *J. Comput. Chem.* **2005**, *26*, 1781–1802.
27. Feller, S. E.; Zhang, Y. H.; Pastor, R. W.; Brooks, B. R. Constant-Pressure Molecular-Dynamics Simulation—The Langevin Piston Method. *J. Chem. Phys.* **1995**, *103*, 4613–4621.
28. Martyna, G. J.; Tobias, D. J.; Klein, M. L. Constant-Pressure Molecular-Dynamics Algorithms. *J. Chem. Phys.* **1994**, *101*, 4177–4189.
29. Jorgensen, W. L.; Chandrasekhar, J.; Madura, J. D.; Impey, R. W.; Klein, M. L. Comparison of Simple Potential Functions for Simulating Liquid Water. *J. Chem. Phys.* **1983**, *79*, 926–935.
30. Andersen, H. C. Rattle—A Velocity Version of The Shake Algorithm for Molecular-Dynamics Calculations. *J. Comput. Phys.* **1983**, *52*, 24–34.
31. Ryckaert, J. P.; Ciccotti, G.; Berendsen, H. J. C. Numerical-Integration of Cartesian Equations of Motion of a System with Constraints—Molecular-Dynamics of *n*-Alkanes. *J. Comput. Phys.* **1977**, *23*, 327–341.
32. Luzar, A.; Chandler, D. Effect of Environment on Hydrogen Bond Dynamics in Liquid Water. *Phys. Rev. Lett.* **1996**, *76*, 928–931.